

ORIGINAL ARTICLE

⁸⁹Zr-pembrolizumab imaging as a non-invasive approach to assess clinical response to PD-1 blockade in cancer

I. C. Kok¹, J. S. Hooiveld^{1†}, P. P. van de Donk^{1†}, D. Giesen¹, E. L. van der Veen², M. N. Lub-de Hooge², A. H. Brouwers³, T. J. N. Hiltermann⁴, A. J. van der Wekken⁴, L. B. M. Hijmering-Kappelle⁴, W. Timens⁵, S. G. Elias⁶, G. A. P. Hospers¹, H. J. M. Groen⁴, W. Uytendil⁷, B. van der Hiel⁸, J. B. Haanen⁷, D. J. A. de Groot¹, M. Jalving¹ & E. G. E. de Vries^{1*}

Departments of ¹Medical Oncology; ²Clinical Pharmacy and Pharmacology; ³Medical Imaging Center; ⁴Pulmonary Medicine; ⁵Pathology and Medical Biology, University Medical Center Groningen, University of Groningen, Groningen; ⁶Department of Epidemiology, Julius Center for Health Sciences and Primary Care, University Medical Center Utrecht, Utrecht University, Utrecht; Departments of ⁷Medical Oncology; ⁸Nuclear Medicine, Netherlands Cancer Institute, Amsterdam, The Netherlands



Available online 1 November 2021

Background: Programmed cell death protein 1 (PD-1) antibody treatment is standard of care for melanoma and non-small-cell lung cancer (NSCLC). Accurately predicting which patients will benefit is currently not possible. Tumor uptake and biodistribution of the PD-1 antibody might play a role. Therefore, we carried out a positron emission tomography (PET) imaging study with zirconium-89 (⁸⁹Zr)-labeled pembrolizumab before PD-1 antibody treatment.

Patients and methods: Patients with advanced or metastatic melanoma or NSCLC received 37 MBq (1 mCi) ⁸⁹Zr-pembrolizumab (~2.5 mg antibody) intravenously plus 2.5 or 7.5 mg unlabeled pembrolizumab. After that, up to three PET scans were carried out on days 2, 4, and 7. Next, PD-1 antibody treatment was initiated. ⁸⁹Zr-pembrolizumab tumor uptake was calculated as maximum standardized uptake value (SUV_{max}) and expressed as geometric mean. Normal organ uptake was calculated as SUV_{mean} and expressed as a mean. Tumor response was assessed according to (i)RECIST v1.1.

Results: Eighteen patients, 11 with melanoma and 7 with NSCLC, were included. The optimal dose was 5 mg pembrolizumab, and the optimal time point for PET scanning was day 7. The tumor SUV_{max} did not differ between melanoma and NSCLC (4.9 and 6.5, *P* = 0.49). Tumor ⁸⁹Zr-pembrolizumab uptake correlated with tumor response (*P* trend = 0.014) and progression-free (*P* = 0.0025) and overall survival (*P* = 0.026). ⁸⁹Zr-pembrolizumab uptake at 5 mg was highest in the spleen with a mean SUV_{mean} of 5.8 (standard deviation ±1.8). There was also ⁸⁹Zr-pembrolizumab uptake in Waldeyer's ring, in normal lymph nodes, and at sites of inflammation.

Conclusion: ⁸⁹Zr-pembrolizumab uptake in tumor lesions correlated with treatment response and patient survival. ⁸⁹Zr-pembrolizumab also showed uptake in lymphoid tissues and at sites of inflammation.

Key words: pembrolizumab, ⁸⁹Zr, PET, immunotherapy, PD-1

INTRODUCTION

Immune checkpoint blockade with monoclonal antibodies targeting programmed cell death protein 1 (PD-1), such as pembrolizumab, is a standard of care for numerous tumor types, including melanoma and non-small-cell lung cancer (NSCLC).^{1,2} However, only a subset of treated patients respond to this therapy, while all patients are at risk for treatment-induced side-effects.³ Immunohistochemical

programmed death-ligand 1 (PD-L1) expression in the tumor is a predictive biomarker for patients with NSCLC.⁴ However, not all patients with high tumor PD-L1 expression respond to PD-1 blockade.^{5,6} Moreover, patients lacking immunohistochemical tumor PD-L1 expression can still experience treatment benefit from PD-1 blockade. The Food and Drug Administration also approved pembrolizumab for adults and children with tumor mutational burden-high solid tumors.⁷ However, again, not all patients with such a high mutational burden will respond. For melanoma, no approved companion diagnostic for patient selection is available.

There are likely multiple factors involved in tumor response to PD-1 antibodies, including PD-1 expression by tumor-infiltrating T cells and the amount of PD-1 antibody reaching its target. Molecular imaging using a radiolabeled

*Correspondence to: Dr Elisabeth G. E. de Vries, Department of Medical Oncology, University Medical Center Groningen, Hanzeplein 1, PO Box 30.001, 9700 RB, Groningen, The Netherlands. Tel: +31-503612821; Fax: +31-503614862

E-mail: e.g.e.de.vries@umcg.nl (E. G. E. de Vries).

†These authors contributed equally.

0923-7534/© 2022 The Authors. Published by Elsevier Ltd on behalf of European Society for Medical Oncology. This is an open access article under the CC BY license (<http://creativecommons.org/licenses/by/4.0/>).

antibody and positron emission tomography (PET) can provide insight into these aspects by giving non-invasive whole-body information.

The impact of PD-1 differs between tumor types. CD8 and PD-1 RNA expression by tumor-infiltrating T cells appear to be better determinants of response to immune checkpoint inhibitors in patients with melanoma than in patients with NSCLC.⁸ Therefore, it is interesting to explore whether the uptake of PD-1 antibody varies between tumor types. Moreover, imaging with a PD-1 antibody will provide information about its biodistribution and uptake by the immune system, which is currently unknown.

Therefore, we carried out a study with zirconium-89 (⁸⁹Zr)-pembrolizumab in patients with locally advanced or metastatic melanoma and NSCLC. The aim was to assess ⁸⁹Zr-pembrolizumab tumor uptake and whole-body biodistribution before treatment with a PD-1 antibody and explore its relationship with patient outcome.

PATIENTS AND METHODS

Patient population

Patients with histologically or cytologically documented locally advanced or metastatic melanoma or NSCLC, eligible for PD-1 antibody treatment, were included. Other inclusion criteria were age ≥ 18 years, Eastern Cooperative Oncology Group performance status of 0-1, ability to comply with protocol, life expectancy ≥ 12 weeks, and RECIST v1.1 measurable disease.⁹ The study was approved by the Medical Ethical Committee of the University Medical Center Groningen (UMCG) and registered with [ClinicalTrials.gov](https://clinicaltrials.gov/ct2/show/study/NCT02760225) (NCT02760225). All patients gave written informed consent. All procedures carried out in the study involving human participants were in accordance with the ethical standards of the institutional and/or national research committee and with the 1964 Helsinki declaration and its later amendments or comparable ethical standards.

Study design

This two-center study was carried out in the UMCG and the Netherlands Cancer Institute-Antoni van Leeuwenhoek Hospital (NKI-AvL). The study contained two parts, parts A and B. In part A, the optimal tracer protein dose of ⁸⁹Zr-pembrolizumab and the optimal time point for PET imaging were assessed. Patients received ~ 2.5 mg pembrolizumab labeled with 37 MBq (1 mCi) ⁸⁹Zr-oxalate intravenously, combined with 2.5 mg or 7.5 mg unlabeled pembrolizumab, resulting in a total dose of 5 or 10 mg. These two doses were based on the pharmacokinetic results of a phase I study with pembrolizumab.¹⁰ ⁸⁹Zr-pembrolizumab PET scans were carried out on days 2, 4, and 7 after tracer injection. The unlabeled antibody dose was considered sufficient when the mean standardized uptake value (SUV_{mean}) in the blood pool on day 4 was comparable to other ⁸⁹Zr-monoclonal antibodies with well-known kinetics over time.^{11,12} In part B, PET imaging was carried out at the optimal

pembrolizumab dose and day of imaging as determined in part A.

When feasible, a tumor biopsy was carried out in part B shortly after the day 7 PET scan. Participation in the ⁸⁹Zr-pembrolizumab PET imaging study was followed by PD-1 antibody treatment as per standard of care (pembrolizumab or nivolumab \pm ipilimumab). Tumor response assessment was carried out every 12 weeks from the start of treatment, according to RECIST v1.1, and when applicable, iRECIST.⁹

⁸⁹Zr-pembrolizumab PET scanning

⁸⁹Zr-pembrolizumab was produced as described previously.¹³ PET scans were combined with a low-dose computed tomography (CT) scan for attenuation correction and anatomic reference. In the UMCG, PET scans were carried out with a Biograph mCT 64-slice PET/CT camera or a Biograph mCT 40-slice PET/CT camera [both Siemens (Siemens Healthcare, Erlangen, Germany)] and in the NKI-AvL with a Philips (Philips Medical Systems, Best, The Netherlands) GEMINI TF Big Bore, 16-slice PET/CT camera. PET acquisitions on days 2 and 4 were carried out from head to upper thigh in up to six bed positions with 5 min/bed position and the legs in up to nine bed positions with 2 min/bed position. Day 7 post-injection head to upper thigh was scanned in up to six bed positions with 10 min/bed position and the legs in up to nine bed positions with 4 min/bed position. All PET images were reconstructed using the algorithm for multicenter ⁸⁹Zr-monoclonal antibody PET scan trials.¹⁴ Image analysis was executed using the Accurate tool (IDL version 8.4; Harris Geospatial Solutions, Bloomfield, NJ) for volume-of-interest (VOI)-based background and lesion analysis.¹⁵ Firstly, when in the field of view, the tumor lesions were identified on a contrast-enhanced baseline CT of the chest and abdomen and contrast-enhanced CT or magnetic resonance imaging of the head. Secondly, spherical VOIs, encompassing each whole tumor lesion, were placed on the ⁸⁹Zr-pembrolizumab PET/low-dose CT around all lesions identified on the diagnostic baseline CT. For normal organ biodistribution measurements, spherical VOIs with fixed sizes per organ were drawn. Bodyweight-corrected SUVs were calculated using the amount of injected activity, body weight, and the amount of radioactivity detected within a VOI. We report the SUV_{max} for tumor lesions and the SUV_{mean} for normal organ ⁸⁹Zr-pembrolizumab uptake. ⁸⁹Zr-pembrolizumab uptake in non-malignant lymph nodes and Waldeyer's ring was compared qualitatively to the surrounding tissue uptake at day 7 post-injection.

Other study assessments

Available archival tumor tissues, obtained within 50 weeks before ⁸⁹Zr-pembrolizumab administration, were collected. Fresh tumor biopsies obtained after the last PET scan were formalin-fixed and paraffin-embedded. Tumor tissue sections of 4 μ m were stained with hematoxylin–eosin and immunohistochemically for PD-1, PD-L1, and CD8.

PD-1 expression was determined with the anti-PD-1 antibody ERP4877(2) (Abcam) as described previously,¹³ with a few modifications to increase signal-to-background ratio. PD-L1 expression was assessed with the anti-PD-L1 SP263 clone (Ventana Medical Systems) and CD8 with the mouse CD8 monoclonal antibody C4/144B (DAKO/Agilent), all according to the manufacturer's protocols. Human tonsil sections served as a positive control for PD-1 and PD-L1 expression. For PD-L1, the percentage of tumor cells with PD-L1-positive membrane staining, at any intensity, was estimated and classified as 0%, <1%, 1%-49%, ≥50%. PD-1 was scored as present or absent in the tumor area. CD8 was scored as negative 0, sporadic 1+, average 2+, abundant 3+ within tumor cell areas, and separately in the stroma directly surrounding the tumor.

⁸⁹Zr-pembrolizumab binding kinetics was determined by studying the accumulation and dissociation of PD-1-bound ⁸⁹Zr-pembrolizumab in peripheral blood mononuclear cells (PBMCs) with a radioactive binding assay (Supplementary Methods, available at <https://doi.org/10.1016/j.annonc.2021.10.213>). The PBMCs were pre-stimulated with phytohemagglutinin and interleukin-2 to increase PD-1 expression (Supplementary Figure S1, available at <https://doi.org/10.1016/j.annonc.2021.10.213>). Internalization of pembrolizumab, chelator-conjugated (pembrolizumab-N-succinyl desferal; pembrolizumab-N-sucDf), pembrolizumab-N-sucDf, and the anti-PD-1-antibody nivolumab was assessed in PD-1-expressing PBMC flow cytometrically (Supplementary Methods, available at <https://doi.org/10.1016/j.annonc.2021.10.213>).

Statistical analyses

We used standard descriptive statistics to report patient characteristics. PET analyses were primarily carried out for all tumor lesions and after excluding small lesions (defined as tumor lesions with a long axis <1 cm and malignant lymph nodes with a short axis <1 cm) to take partial volume effects into account.¹⁶ Previously irradiated lesions were excluded. To study ⁸⁹Zr-pembrolizumab tumor uptake in relation to time post-injection, primary tumor type, metastatic site, immunohistochemistry (PD-1, PD-L1 CD8), and best tumor response at a patient level, we used linear mixed-effect models with the natural logarithm of SUV_{max} as dependent variable to account for its right-skewed distribution and using random intercepts to account for within-patient clustering of data (and, if applicable, within-tumor clustering). From these models, we report geometric mean SUV_{max} values and corresponding 95% confidence intervals (CIs) and Wald *P* values, after back transformation of the estimated mean ln(SUV_{max}), using Satterthwaite's degrees of freedom approximation and restricted maximum likelihood. Likelihood ratio *P* values were obtained under maximum likelihood. We used Akaike's information criterion to select the best fitting time post-injection versus tumor uptake curve from a linear, log-linear, or quadratic fit. We similarly assessed tumor-to-background uptake ratios and the biodistribution in normal tissues using SUV_{mean} as the

dependent variable (the latter without natural logarithmic transformation due to its approximate normal distribution). These time–activity curves were assessed in cohort A, adjusted for the tracer dose, and projected at the 5-mg dose level. All other analyses were carried out in cohorts A and B combined.

Finally, to explore the relationship between per-patient geometric mean pre-treatment ⁸⁹Zr-pembrolizumab tumor uptake and progression-free survival (PFS) and overall survival (OS), we used Cox regression with Firth's bias correction for small samples. For this, we analyzed per-patient geometric mean tumor SUV_{max} continuously, assuming linearity and binning patients in above and below median uptake groups.

All reported *P* values are two-sided, and we used R version 3.2.1 (www.r-project.org) for macOS for analyses, particularly using packages lme4 (1.1-11), lmerTest (2.0-20), and coxphf (1.11).

RESULTS

Eighteen patients were enrolled between October 2016 and January 2019, 6 patients in part A, 12 in part B, 11 with metastatic melanoma, and 7 with metastatic NSCLC. Patient characteristics are shown in Table 1. With data cut-off set at 27 January 2021, their median follow-up was 22 months (range: 4-50+ months). No tracer-related adverse events were observed following ⁸⁹Zr-pembrolizumab administration.

Dose finding and imaging time point for ⁸⁹Zr-pembrolizumab PET

In part A, the first two patients received 2.5 mg ⁸⁹Zr-pembrolizumab plus 7.5 mg unlabeled pembrolizumab. This resulted in an SUV_{mean} in the blood pool of 6.7 and 8.4 on day 2, 5.6 and 7.8 on day 4, and 4.0 and 5.3 on day 7 post-injection. The next four patients in cohort A received 2.5 mg ⁸⁹Zr-pembrolizumab plus 2.5 mg unlabeled pembrolizumab, resulting in a median SUV_{mean} in the blood pool of 8.7 (range: 8.1-9.6), 6.4 (5.4-7.0), and 4.5 (4.2-7.5) on days 2, 4, and 7 post-injection, respectively.

Table 1. Patient characteristics

Total number of patients	18
Median age, years (range)	55.3 (24.9-72.7)
Sex, <i>n</i> (%)	
Male	10 (56)
Female	8 (44)
Primary tumor, <i>n</i> (%)	
NSCLC	7 (39)
Melanoma	11 (61)
ECOG performance status, <i>n</i> (%)	
0	11 (61)
1	7 (39)
Number of lines of therapy, <i>n</i> (%)	
0	15 (83)
1	3 (17)

ECOG, Eastern Cooperative Oncology Group; NSCLC, non-small-cell lung cancer.

The six patients in part A had 35 tumor lesions, of which 5 were previously irradiated bone metastases. In the 30 non-irradiated lesions, the geometric mean SUV_{max} increased from day 2 to 7, from 5.1 (95% CI 3.0-8.6) to 6.7 (95% CI 3.9-11.3) (Figure 1A; adjusted for dose and projected at 5 mg). The two most frequent metastatic sites were lung ($n = 16$ lesions, five patients) and bone ($n = 5$ lesions, three patients). The increasing tumor-to-blood ratio from day 2 to 7 for all 30 lesions and lung and bone metastasis separately is shown in Figure 1B. Altogether, the 5-mg protein dose for ^{89}Zr -pembrolizumab in part B was determined to be superior to the 10-mg dose. The optimal time point, given the highest tumor-to-blood ratio, for PET imaging was day 7.

^{89}Zr -pembrolizumab biodistribution

^{89}Zr -pembrolizumab uptake measured over time, as carried out in cohort A, was low in the brain, lung, bone cortex, subcutaneous tissue, and the abdominal cavity (Figure 1C and D). The 16 patients receiving 5 mg pembrolizumab showed high spleen and bone marrow uptake with a mean SUV_{mean} of 5.8 ± 1.8 and 2.4 ± 0.9 on day 7, respectively. There was also ^{89}Zr -pembrolizumab uptake in the liver and kidneys (Supplementary Table S1, available at <https://doi.org/10.1016/j.annonc.2021.10.213>).

Uptake in the spleen increased from day 2 to 7, while uptake in the blood pool decreased, indicating specific ^{89}Zr -pembrolizumab uptake (Figure 1C and D). In 12 patients, there was clear uptake in Waldeyer's ring, and in 6 patients in normal lymph nodes (Supplementary Figure S2, available at <https://doi.org/10.1016/j.annonc.2021.10.213>). Moreover, ^{89}Zr -pembrolizumab uptake was visually present at sites of inflammation, due to autoimmune disease, prior surgery, and infection (Supplementary Figure S3, available at <https://doi.org/10.1016/j.annonc.2021.10.213>). No clear tracer uptake was seen in the tissues where four patients later experienced an immune-related adverse event to anti-PD-1 antibody therapy.

^{89}Zr -pembrolizumab tumor uptake

Combining data from cohorts A and B, a total of 103 non-irradiated tumor lesions in 18 patients were analyzed. Tracer uptake in tumor lesions ranged from 0.08 to 34.5 SUV_{max} . Uptake in tumor lesions varied between and sometimes also within patients (Figure 2). ^{89}Zr -pembrolizumab uptake did not differ between patients with NSCLC and melanoma (geometric mean SUV_{max} of 6.5, 95% CI 3.4-12.5, $n = 45$ lesions versus 4.9, 95% CI 2.8-8.4, $n = 58$ lesions; $P = 0.49$; Figure 3B).

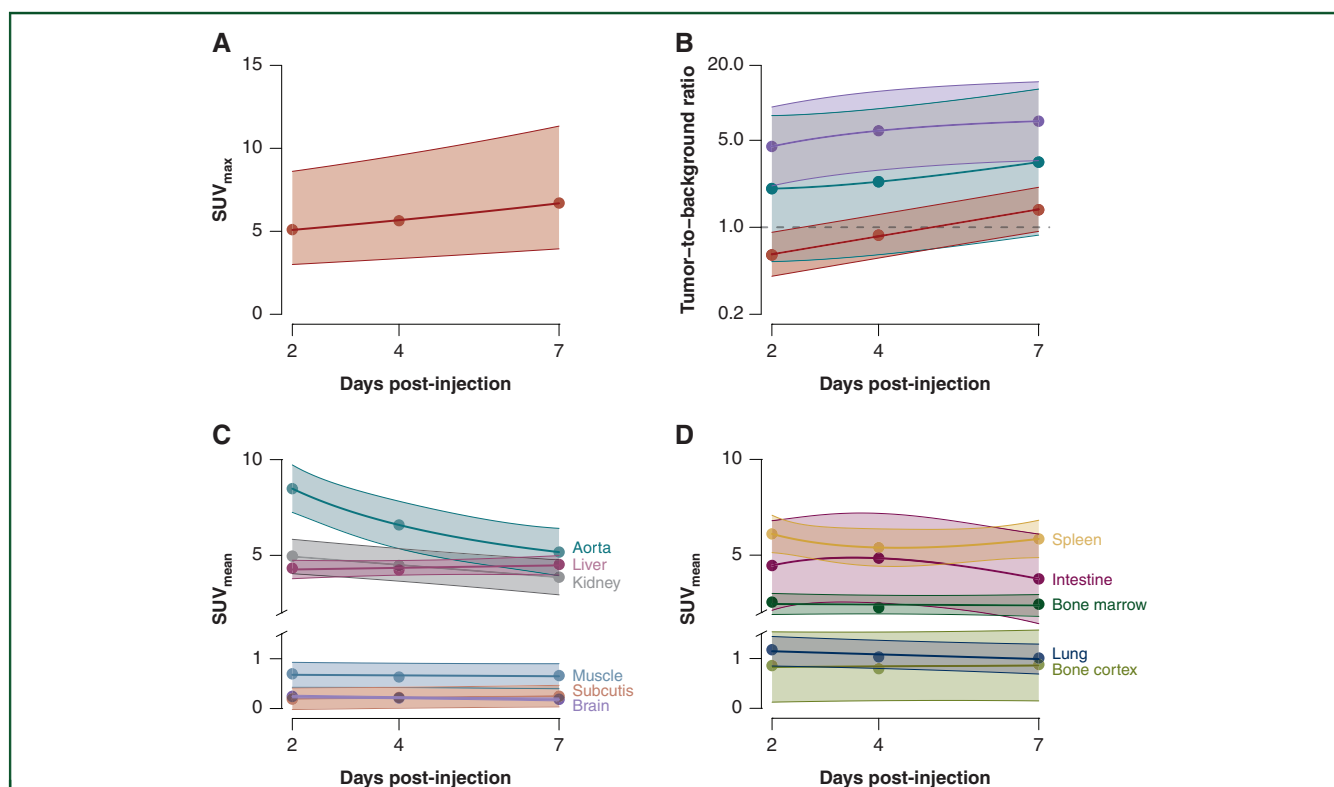


Figure 1. ^{89}Zr -pembrolizumab positron emission tomography (PET) biodistribution.

(A) ^{89}Zr -pembrolizumab tumor uptake [geometric mean maximum standardized uptake value (SUV_{max}), 95% confidence interval (CI)] of patients imaged within cohort A ($n = 6$ patients, 30 lesions) adjusted for pre-dose and projected to 5 mg total protein dose according to time post-injection. (B) The geometric mean tumor SUV_{max} -to-background SUV_{mean} ratio of lung metastases (purple, $n = 16$; five patients), bone metastases (teal, $n = 5$; three patients), and tumor-to-blood ratio (red, $n = 30$; six patients), adjusted for dose and projected to 5 mg total protein dose according to time post-injection. Lines represent fitted regression lines accompanied by 95% CI bands. (C and D) Two graphs showing ^{89}Zr -pembrolizumab tracer uptake [mean SUV_{mean} (95% CI)] in healthy tissues at 2, 4, and 7 days after tracer injection of six patients. Two patients received 10 mg tracer and four patients 5 mg tracer. Tracer uptake (SUV_{mean}) is adjusted for total protein dose and extrapolated to the 5-mg total protein dose level.

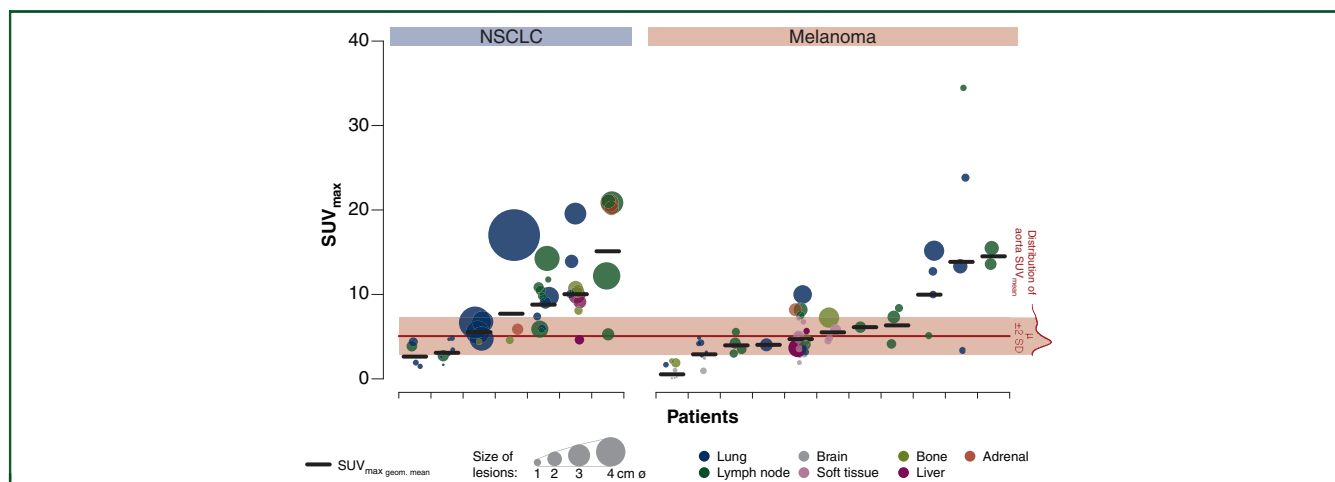


Figure 2. ^{89}Zr -pembrolizumab tumor uptake for the 103 lesions expressed as maximum standardized uptake value (SUV_{max}) on day 7 positron emission tomography (PET) scan, depicted per patient ($n = 18$).

Patients are categorized per tumor type and ordered according to increasing geometric mean tumor SUV_{max} per patient (horizontal black lines). Each tumor lesion is one circle, with the circle size corresponding to computed tomography (CT)-derived lesion size and color depicting lesion location. NSCLC, non-small-cell lung cancer; SD, standard deviation.

^{89}Zr -pembrolizumab tumor uptake was strongly related to the lesion site ($P = 0.000019$), with lymph node metastases showing the highest uptake with a geometric

mean SUV_{max} of 6.7 (95% CI 4.4-10.4), and brain metastases the lowest with a geometric mean SUV_{max} of 1.9 (95% CI 1.1-3.3) (Figure 3C). Examples of

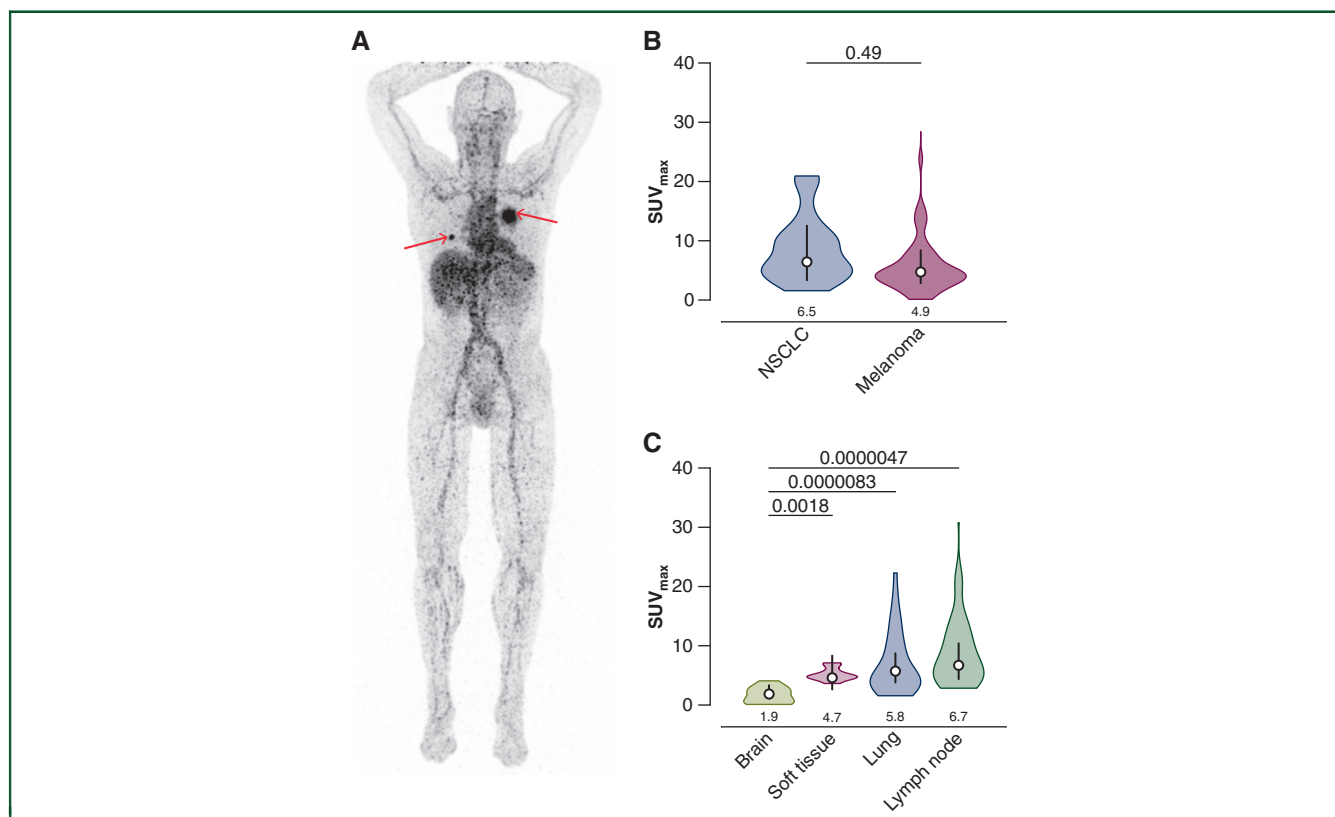


Figure 3. ^{89}Zr -pembrolizumab tumor uptake on day 7.

(A) Maximum intensity projection of ^{89}Zr -pembrolizumab positron emission tomography (PET) scan 7 days after tracer injection; red arrows indicate tumor lesions. (B) Violin plot of the distribution of tumor maximum standardized uptake value (SUV_{max}) day 7 according to primary tumor type with bottom and top 1% of SUV_{max} values truncated (1st, 50th, and 99th SUV_{max} percentile: 1.6, 6.8, 21.0 for non-small-cell lung cancer (NSCLC) and 0.1, 4.4, 28.4 for melanoma); black vertical lines are 95% confidence intervals (CIs) of geometric mean SUV_{max} ; white dots within black lines and values below the violin plot are the actual geometric means; two-sided Wald P values for geometric mean SUV_{max} comparison between tumor types above the graph; NSCLC: 45 lesions in 7 patients, melanoma: 58 lesions in 11 patients. (C) Violin plot of the distribution of tumor SUV_{max} according to lesion site for sites with at least 10 observations with bottom and top 1% of SUV_{max} values truncated (1st, 50th, and 99th SUV_{max} percentile: 0.1, 1.5, 4.1 for the brain; 3.6, 4.9, 7.1 for soft tissue; 1.5, 4.8, 22.3 for lung; 2.8, 7.4, 30.8 for lymph node); otherwise representation as for panel B; brain: 10 lesions in 3 patients, soft tissue: 10 lesions in 1 patient, lung/pleural: 37 lesions in 4 patients, lymph node: 28 lesions in 10 patients. Likelihood ratio test for the overall effect of lesion site on geometric mean SUV_{max} $P = 0.000019$.

^{89}Zr -pembrolizumab tumor uptake on PET are shown in [Supplementary Figure S4](https://doi.org/10.1016/j.annonc.2021.10.213), available at <https://doi.org/10.1016/j.annonc.2021.10.213>.

Exclusion of small lesions ($n = 30$) yielded overall higher geometric mean SUV_{max} estimates but did not substantially change the relationship between uptake and tumor type or metastatic site described above (data not shown).

^{89}Zr -pembrolizumab PET uptake and response to therapy

Fourteen patients received pembrolizumab 2 mg/kg in a 3-weekly schedule and two patients received nivolumab 240 mg every 2 weeks. One patient with NSCLC received three cycles of pembrolizumab, followed by nivolumab. One patient with melanoma received ipilimumab 3 mg/kg and nivolumab 1 mg/kg every 3 weeks until cycle 4, followed by nivolumab monotherapy, 240 mg every 2 weeks. The three patients with brain metastases received radiotherapy shortly after the initiation of immunotherapy. Median treatment duration was 177 days (range: 21-717 days) overall, 185 days (range: 21-589 days) in patients with melanoma, and 119 days (range: 87-717 days) in patients with NSCLC. At the end of follow-up, all patients were off treatment. Eight patients were alive, of whom three were without evidence of disease. Treatment response and reasons for termination of immunotherapy are shown in [Table 2](#). The median follow-up time of the eight patients alive at data cut-off was 34 months (range: 22-50+ months).

The geometric mean SUV_{max} of the 103 tumor lesions was positively associated with tumor response (P for trend = 0.014; [Figure 4A](#)) and target lesion size change ([Figure 4B](#)). Patients with a high geometric mean ^{89}Zr -pembrolizumab uptake (above the median of 5.8) showed a longer PFS and OS than patients with low uptake ($P = 0.0025$ and $P = 0.026$, respectively; [Figure 4C](#) and [D](#)). One of the two patients with high ^{89}Zr -pembrolizumab uptake who died during follow-up experienced a partial response. However, this patient died 21 months after starting pembrolizumab treatment due to pembrolizumab-induced antiphospholipid syndrome, with intestinal ischemia and respiratory failure due to pneumonitis. When analyzed continuously, the hazard ratio for PFS for each unit decrease in geometric mean SUV_{max} per patient was 1.22 (95% CI 1.05-1.48; $P = 0.0097$), and 1.13 (95% CI 0.97-1.34; $P =$

0.13) for OS. The exclusion of small lesions did not substantially change the above-described relationship between uptake and patient outcome (data not shown).

Other study assessments

Tumor samples of 13 patients were analyzed immunohistochemically, 10 were archival tissues, and 3 fresh tumor biopsies were taken after the last ^{89}Zr -pembrolizumab PET scan. PD-1 expression was found in five samples. In these PD-1-positive samples, CD8 expression was also observed. Results are shown in [Supplementary Table S2](#), available at <https://doi.org/10.1016/j.annonc.2021.10.213>. Three of the PD-1-positive tumor tissues expressed PD-L1. PD-1 expression assessed immunohistochemically did not correlate with the geometric mean SUV_{max} ^{89}Zr -pembrolizumab uptake of that patient ([Supplementary Figure S5](#), available at <https://doi.org/10.1016/j.annonc.2021.10.213>). Of the three fresh tumor biopsy samples, two contained enough tissue to assess PD-1 expression. Both lesions showed high uptake on the ^{89}Zr -pembrolizumab PET scan (SUV_{max} 17.0 and 21.0), but were negative for PD-1 expression measured immunohistochemically.

Small amounts of ^{89}Zr -pembrolizumab accumulated in PD-1-expressing PBMCs; hence dissociation of PD-1-bound tracer occurred ([Supplementary Figure S1](#), available at <https://doi.org/10.1016/j.annonc.2021.10.213>). Pembrolizumab showed modest internalization in pre-stimulated, PD-1-expressing PBMCs with 13.6% ($\pm 10.7\%$) after 2-h incubation ([Supplementary Figure S1](#), available at <https://doi.org/10.1016/j.annonc.2021.10.213>). Pembrolizumab internalization was not affected by antibody conjugation. Internalization rates for pembrolizumab and nivolumab, which target distinct epitopes of PD-1, with different affinities, were comparable.¹⁷

DISCUSSION

In this study, we demonstrate that ^{89}Zr -pembrolizumab PET imaging is a safe and non-invasive imaging modality for whole-body visualization of PD-1 and pembrolizumab biodistribution. Tumor ^{89}Zr -pembrolizumab uptake correlated with tumor response, PFS, and OS. ^{89}Zr -pembrolizumab uptake was also seen in lymphoid tissues reflecting the presence of PD-1 in normal tissues and at sites of inflammation. These findings illustrate that all major sites for T cells are visualized with ^{89}Zr -pembrolizumab PET imaging.

^{89}Zr -labeled anti-PD-1 antibody nivolumab was studied in 13 patients with NSCLC.¹⁸ They report higher ^{89}Zr -nivolumab uptake in tumor lesions responding to nivolumab treatment. However, they only report response for individual tumor lesions and not for the patient as a whole. Recently, another study using ^{89}Zr -pembrolizumab was published performing PET scans in 12 patients with NSCLC before pembrolizumab monotherapy.¹⁹ This study implemented a different dosing strategy by administering a labeled dose of 2 mg without adding any unlabeled pembrolizumab. Fourteen days later, 2 mg labeled ^{89}Zr -pembrolizumab was administered on the same day as the first

Table 2. Achieved tumor response and reason for stopping PD-1 antibody

Patients with melanoma, n (%)	
Complete response	3 (27)
Partial response	3 (27)
Stable disease	2 (18)
Progressive disease	3 (27)
Patients with NSCLC, n (%)	
Complete response	0 (0)
Partial response	3 (43)
Stable disease	1 (14)
Progressive disease	3 (43)
Reason for termination of treatment, n (%)	
Progressive disease	9 (50)
Completed treatment	5 (28)
Immune-related toxicity	4 (22)

NSCLC, non-small-cell lung cancer; PD-1, programmed cell death protein 1.

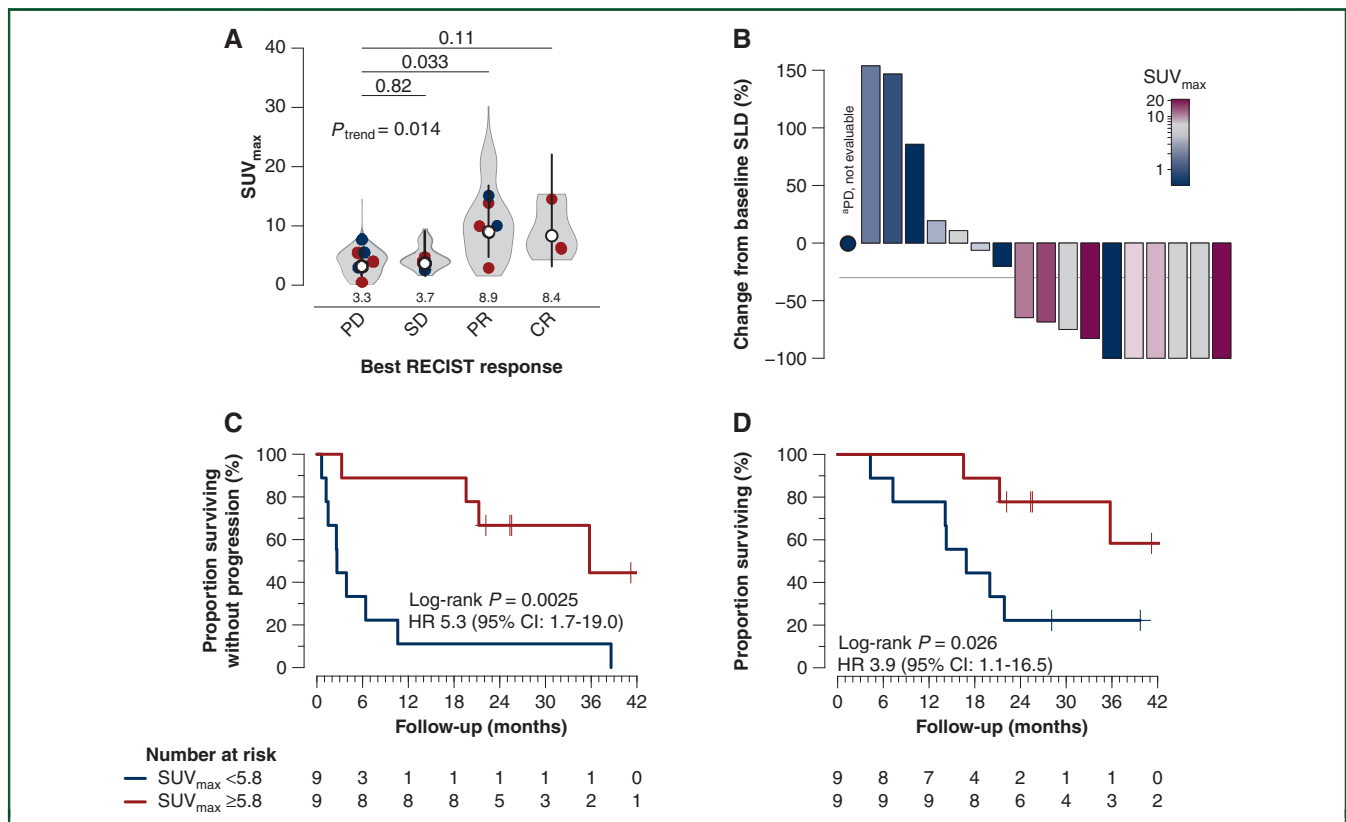


Figure 4. ⁸⁹Zr-pembrolizumab tumor uptake and clinical outcome measures.

(A) ⁸⁹Zr-pembrolizumab tumor uptake as geometric mean maximum standardized uptake value (SUV_{max}) on day 7 and best tumor response (n = 18 patients). Gray violin plot areas show the distribution of SUV_{max} at the tumor level per best response category, with bottom and top 1% values truncated [1st, 50th, and 99th SUV_{max} percentile: 0.1, 4.4, 14.5 for progressive disease (PD); 1.6, 4.2, 9.5 for stable disease (SD); 1.6, 9.9, 30.2 for partial response (PR); 4.2, 7.9, 15.4 for complete response (CR)]; points show geometric mean uptake per patient, with colors indicating tumor type [red, melanoma; dark blue, non-small-cell lung cancer (NSCLC)]; black vertical lines are 95% confidence intervals (CIs) of geometric mean SUV_{max}, and white dots within black lines and values below the violin plot are the actual geometric means; with two-sided Wald P values, supplemented with a two-sided likelihood ratio P for trend; PD = 27 lesions in six patients, SD = 29 in three patients, PR = 41 in six patients, CR = 6 in three patients. (B) Waterfall plots depicting percentage change in sum of longest diameters of the target lesions (SLD) from baseline [measured on computed tomography (CT)], with color scale indicating geometric mean SUV_{max} of the tumor lesions per patient; ^aindicates patient with PD, however no SLD change data are available. (C) Progression-free survival according to geometric mean tumor SUV_{max} per patient (red depicts the group above and dark blue the group below the median geometric mean uptake of an SUV_{max} of 5.8). (D) Overall survival of the patients binned and represented as in panel C (red depicts the group above and dark blue the group below the median geometric mean uptake of an SUV_{max} of 5.8).

full therapeutic dose of 200 mg pembrolizumab. The 2-mg labeled dose alone suffers from fast clearance and early trapping in sink organs, whereas the 200-mg unlabeled pembrolizumab pre-dose resulted in low uptake in tumor lesions likely due to saturation. This study observed a trend between tracer uptake in tumor lesions and response to therapy. However, this was not statistically significant. We demonstrate that ⁸⁹Zr-pembrolizumab uptake in tumor lesions correlates not only with response to therapy, but also with PFS and OS. Interestingly, for ⁸⁹Zr-atezolizumab targeting PD-L1, we also observed a relationship between tumor ⁸⁹Zr-atezolizumab uptake and response PFS, and OS.¹² Therefore, this is our second study that demonstrates that PET imaging using PD-1 and PD-L1 radiolabeled antibodies may predict response to therapy and survival. Both studies showing these correlations are of modest size. Therefore, whole-body tumor uptake of radiolabeled anti-PD-1 or anti-PD-L1 antibodies deserves to be studied in a larger patient population.

In melanoma, CD8 and PD-1 messenger RNA expression are better determinants of response than in NSCLC.⁸ In our relatively small number of patients with melanoma and

NSCLC, we found similar ⁸⁹Zr-pembrolizumab tumor uptake. We were unable to study the relationship between uptake and patient outcome within primary tumor subtypes due to the limited sample size. The antitumor efficacy of immune checkpoint inhibitors depends on multiple factors. Hence, a future study might also include immune checkpoint inhibitor tumor uptake as a key treatment response factor.

A tracer dose of 5 mg protein in total was found to be sufficient with adequate activity in the blood pool at day 4 post-injection, based on experience with other radiolabeled antibodies.¹¹ In normal tissues, there was a clear ⁸⁹Zr-pembrolizumab uptake in the spleen and bone marrow, and in most patients, uptake in Waldeyer's ring and part of the normal lymph nodes. Information about PD-1 antibody uptake in the lymphoid system was, until now, only available from preclinical studies. In humanized NOG mice engrafted with human CD34+ hematopoietic stem cells and xenografted with human A375M melanoma cells, the highest ⁸⁹Zr-pembrolizumab uptake occurred in the spleen, mesenteric lymph nodes, bone marrow, thymus, and tumor.¹³ In healthy Cynomolgus monkeys, a similar bio-distribution pattern was found with preferential uptake in

lymph nodes, spleen, and tonsils.²⁰ Tracer uptake in malignant lymph nodes was highest of all tumor localizations. Therefore, it might be interesting to evaluate whether ⁸⁹Zr-pembrolizumab PET can distinguish benign from malignant lymph nodes. Our current study was not sufficiently large enough nor designed to address this question, but this may be relevant to assess in a future study.

Other PD-1 PET imaging studies report uptake in the spleen and bone marrow as a readout for the lymphoid system.^{18,19} The ⁸⁹Zr-pembrolizumab study also observed uptake in non-malignant lymph nodes. The SUVs found in the spleen and in the bone marrow were nearly identical and in line with the results of our study.^{18,19} In the ⁸⁹Zr-atezolizumab PET imaging study, tracer uptake was higher in the spleen and bone marrow than ⁸⁹Zr-pembrolizumab with an SUV_{mean} of 14.9 and 3.1, respectively, at day 7 post-injection.¹² This is likely because PD-L1 is next to lymphocytes, also expressed by macrophages, dendritic cells, and endothelial littoral cells in the spleen.

Interestingly, we also show ⁸⁹Zr-pembrolizumab uptake at sites of chronic inflammation, a phenomenon we also found using ⁸⁹Zr-atezolizumab.¹² This is likely the result of the fact that PD-1 and PD-L1 are modulators of the immune response at sites of chronic inflammation.^{21,22}

⁸⁹Zr-pembrolizumab and ⁸⁹Zr-nivolumab seem to demonstrate similar uptake in tumor lesions, spleen, and bone marrow.¹⁸ This occurred despite major differences in their affinity for the PD-1 receptor. Pembrolizumab binds the CD loop of the PD-1 receptor with $K_D = 29$ pM, while nivolumab targets the N-loop epitope with ~ 100 -fold lower binding affinity. Moreover, after the PD-1-bound antibody internalization, ⁸⁹Zr is trapped in the cell. PET imaging at 7 days may, therefore, in part reflect residualized ⁸⁹Zr. We found limited PD-1 expression in unstimulated PBMCs, which moderately increased after stimulation. Pembrolizumab and nivolumab showed comparable binding and internalization in these PD-1-expressing PBMCs. This further supports the result that PET imaging using these immune checkpoint inhibitors is not affected by their different affinities for PD-1.

In the current study, we observed no correlation between lymphocytic markers, such as PD-1 and CD8 expression, and ⁸⁹Zr-pembrolizumab tumor uptake. Interestingly, in other PET imaging studies of immune checkpoint molecules, similar results are found.^{12,18,19} These discordant results between PET imaging and immunohistochemistry are likely due to the heterogeneity of PD-1 expression within and between tumor lesions. A biopsy specimen might not accurately reflect expression levels in all tumor lesions. The heterogeneity of tracer uptake in tumor lesions, as depicted in Figure 2, illustrates this problem. Several studies have found different expression levels of immune checkpoint molecules in different tumor lesions within the same patient.²³⁻²⁶ This further illustrates the possible additive value of whole-body PET scanning versus a tumor biopsy of a part of a single lesion. Limitations of this study are the number of patients included and the limited availability of tumor tissue for immunohistochemical analysis. A larger

and more homogeneous study is required to validate these results. The collection of tumor tissue to correlate PET imaging findings with immunohistochemistry and autoradiography results will aid further validation of this approach.

In summary, this study shows that ⁸⁹Zr-pembrolizumab tumor uptake with PET imaging correlates with response to PD-1 antibody treatment, including PFS and OS. These findings require validation in larger studies to prove their impact on patient selection for PD-1 blockade.

FUNDING

This work was supported by the Dutch Cancer Society Grant POINTING [grant number RUG 2016-10034] and the Innovative Medicines Initiatives2 Joint Undertaking project TRISTAN [grant number GA no. 116106]. This Joint Undertaking receives support from the European Union's Horizon 2020 research and innovation program and EPPIA (no grant number).

DISCLOSURE

MJ reports consultancy fees from AstraZeneca (paid to UMCG). JBH reports consultancy roles for Achilles Therapeutics, BioNTech, BMS, GSK, Immunocore, Instil Bio, Molecular Partners, MSD, Merck Serono, Neogene Therapeutics, Novartis, Pfizer, PokeAcel, Roche/Genentech, Sanofi, T-Knife, and Third Rock Ventures and research grants from Amgen, Asher-Bio, BMS, BioNTech, MSD, Novartis, and Neogene Therapeutics (paid to the Netherlands Cancer Institute). WT reports fees from Merck, Sharp, Dohme, and Bristol-Myers-Squibb (paid to UMCG). EGEDV reports an advisory role at Daiichi Sankyo, NSABP, and Sanofi and research funding from Amgen, AstraZeneca, Bayer, Chugai Pharma, Crescendo, CytomX Therapeutics, G1 Therapeutics, Genentech, Nordic Nanovector, Radius Health, Regeneron, Roche, Servier, and Synthon (paid to UMCG). GAPH reports consulting and advisory role at Amgen, Roche, MSD, BMS, Pfizer, Novartis, and Pierre Fabry and research funding from BMS and Seerave (paid to UMCG). TJNH reports consultancy fees (paid to UMCG) from BMS, MSD, Merck, Boehringer, AstraZeneca, and Roche. AJvdW reports an advisory role at Janssen, Takeda, and Boehringer-Ingelheim (paid to UMCG) and research funding from AstraZeneca, Boehringer-Ingelheim, Pfizer, Roche, and Takeda. MNL-dH reports research funding from Merck, Bayer, and Amgen (paid to UMCG). HJMG reports an advisory role at Eli Lilly, MSD, BMS, and Novartis. All other authors have declared no conflicts of interest.

REFERENCES

- Schmidt EV, Chisamore MJ, Chaney MF, et al. Assessment of clinical activity of PD-1 checkpoint inhibitor combination therapies reported in clinical trials. *JAMA Netw Open*. 2020;3:e1920833.
- Boussiotis VA. Molecular and biochemical aspects of the PD-1 checkpoint pathway. *N Engl J Med*. 2016;375:1767-1778.
- Xu C, Chen YP, Du XJ, et al. Comparative safety of immune checkpoint inhibitors in cancer: systematic review and network meta-analysis. *Br Med J*. 2018;363:k4226.
- Dolled-Filhart M, Roach C, Toland G, et al. Development of a companion diagnostic for pembrolizumab in non-small cell lung cancer

- using immunohistochemistry for programmed death ligand-1. *Arch Pathol Lab Med*. 2016;140:1243-1249.
5. Aguiar PN, De Mello RA, Hall P, Tadokoro H, de Lima Lopes G. PD-L1 expression as a predictive biomarker in advanced non-small-cell lung cancer: updated survival data. *Immunotherapy*. 2017;9:499-506.
 6. Rittmeyer A, Barlesi F, Waterkamp D, et al. Pembrolizumab versus docetaxel in patients with previously treated non-small-cell lung cancer (OAK): a phase 3, open-label, multicentre randomised controlled trial. *Lancet*. 2017;389:255-265.
 7. Marabelle A, Fakih M, Lopez J, et al. Association of tumour mutational burden with outcomes in patients with advanced solid tumours treated with pembrolizumab: prospective biomarker analysis of the multicohort, open-label, phase 2 KEYNOTE-158 study. *Lancet Oncol*. 2020;20:30445-302259.
 8. Lee SJ, Ruppin E. Multiomics prediction of response rates to therapies to inhibit programmed cell death 1 and programmed cell death 1 ligand 1. *JAMA Oncol*. 2019;5:1614-1618.
 9. Seymour L, Bogaerts J, Perrone A, et al. iRECIST: guidelines for response criteria for use in trials testing immunotherapeutics. *Lancet Oncol*. 2017;18:e143-e152.
 10. Patnaik A, Kang SP, Rasco D, et al. Phase I study of pembrolizumab (MK-3475; anti-PD-1 monoclonal antibody) in patients with advanced solid tumors. *Clin Cancer Res*. 2015;21:4286-4293.
 11. Bensch F, Smeenk MM, van Es SC, et al. Comparative biodistribution analysis across four different ⁸⁹Zr-monoclonal antibody tracers—the first step towards an imaging warehouse. *Theranostics*. 2018;8:4295-4304.
 12. Bensch F, van der Veen EL, Lub-de Hooge MN, et al. ⁸⁹Zr-atezolizumab imaging as a non-invasive approach to assess clinical response to PD-L1 blockade in cancer. *Nat Med*. 2018;24:1852-1858.
 13. Van der Veen EL, Giesen D, Pot-de Jong L, Jorritsma-Smit A, de Vries EGE, Lub-de Hooge MN. ⁸⁹Zr-pembrolizumab biodistribution is influenced by PD-1 mediated uptake in lymphoid organs. *J Immunother Cancer*. 2020;8:e000938.
 14. Makris NE, Boellaard R, Visser EP, et al. Multicenter harmonization of ⁸⁹Zr PET/CT performance. *J Nucl Med*. 2014;55:264-267.
 15. Frings V, van Velden FH, Velasquez LM, et al. Repeatability of metabolically active tumor volume measurements with FDG PET/CT in advanced gastrointestinal malignancies: a multicenter study. *Radiology*. 2014;273:539-548.
 16. Gallivanone F, Canevari C, Gianolli L, et al. A partial volume effect correction tailored for ⁸⁹F-FDG-PET oncological studies. *Biomed Res Int*. 2013;2013:780458.
 17. Fessas P, Lee H, Ikemizu S, Janowitz T. A molecular and preclinical comparison of the PD-1-targeted T-cell checkpoint inhibitors nivolumab and pembrolizumab. *Semin Oncol*. 2017;44:136-140.
 18. Niemeijer AN, Leung D, Huisman MC, et al. Whole body PD-1 and PD-L1 positron emission tomography in patients with non-small cell lung cancer. *Nat Commun*. 2018;9:4664.
 19. Niemeijer AN, Oprea Lager DE, Huisman MC, et al. First-in-human study of ⁸⁹Zr-pembrolizumab PET/CT in patients with advanced stage non-small-cell lung cancer. *J Nucl Med*. 2021. <https://doi.org/10.2967/jnumed.121.261926>.
 20. Li W, Wang Y, Rubins D, et al. PET/CT Imaging of ⁸⁹Zr-N-sucDf-pembrolizumab in healthy cynomolgus monkeys. *Mol Imaging Biol*. 2021;23:250-259.
 21. Jubel JM, Barbati ZR, Burger C, Wirtz DC, Schildberg FA. The role of PD-1 in acute and chronic infection. *Front Immunol*. 2020;11:487.
 22. Sharpe AH, Pauken KE. The diverse functions of the PD1 inhibitory pathway. *Nat Rev Immunol*. 2018;18:153-167.
 23. Madore J, Vilain RE, Menzies AM, et al. PD-L1 expression in melanoma shows marked heterogeneity within and between patients: implications for anti-PD-1/PD-L1 clinical trials. *Pigment Cell Melanoma Res*. 2015;28:245-253.
 24. Madore J, Strbenac D, Vilain R, et al. PD-L1 negative status is associated with lower mutation burden, differential expression of immune-related genes, and worse survival in stage III melanoma. *Clin Cancer Res*. 2016;22:3915-3923.
 25. Bassanelli M, Sioletic S, Martini M, et al. Heterogeneity of PD-L1 expression and relationship with biology of NSCLC. *Anticancer Res*. 2018;38:3789-3796.
 26. Haragan A, Field JK, Davies MPA, Escriu C, Gruver A, Gosney JR. Heterogeneity of PD-L1 expression in non-small cell lung cancer: implications for specimen sampling in predicting treatment response. *Lung Cancer*. 2019;134:79-84.